Pharmaceutical Sciences and Drug Design
ISSN: 3062-4428
2025, Volume 5, Page No: 225-241
Copyright CC BY-NC-SA 4.0
Available online at: www.galaxypub.co/page/journals

Galaxy Publication

Galaxy Publication

RASSF1A Enhances Cisplatin Sensitivity in Non-Small Cell Lung Cancer via MAP1S-Dependent Autophagy Activation and Keap1-Nrf2 Pathway Suppression

Chen Wei[1]*, Rui Huang[1]

[1]Department of Pharmacognosy, Faculty of Pharmacy, Zhejiang University, Hangzhou, China.

* **E-mail** ✉ chen.wei.cn@gmail.com

Received: 11 August 2025; **Revised:** 06 November 2025; **Accepted:** 11 November 2025

ABSTRACT

Cisplatin (DDP) remains a primary chemotherapeutic agent for treating non-small cell lung cancer (NSCLC), but the development of drug resistance limits its clinical efficacy. This study aimed to explore the role of RASSF1A in modulating DDP resistance in NSCLC and to elucidate the underlying molecular mechanisms. Expression levels of RASSF1A and microtubule-associated protein 1S (MAP1S) were assessed using qRT-PCR and Western blotting, while their interaction was verified by co-immunoprecipitation (Co-IP). The half-maximal inhibitory concentration (IC50) of DDP was determined for A549 and DDP-resistant A549/DDP cells. A549/DDP cells were transfected with pCDNA3.1-RASSF1A, pCDNA3.1-MAP1S, or si-RASSF1A and subsequently treated with DDP. Cell viability was evaluated using CCK-8 and 5-ethynyl-2′-deoxyuridine (EDU) assays. Autophagy-related protein levels, including p62, LC3I, and LC3II, were measured via Western blot, and GFP-LC3 puncta formation was examined using immunofluorescence. Additionally, a xenograft mouse model was established using A549/DDP cells to validate in vivo effects. Both RASSF1A and MAP1S were downregulated in NSCLC tissues and displayed a positive correlation. Overexpression of RASSF1A or MAP1S in A549 and A549/DDP cells enhanced DDP-induced cytotoxicity and increased autophagic activity. Mechanistic studies revealed that RASSF1A regulates MAP1S to inhibit the Keap1-Nrf2 pathway, thereby promoting autophagy and improving chemosensitivity. These effects were further corroborated in the in vivo xenograft model. RASSF1A enhances the sensitivity of NSCLC cells to cisplatin by promoting autophagy through MAP1S-mediated inhibition of the Keap1-Nrf2 pathway, offering potential insights for overcoming chemotherapy resistance.

Keywords: RASSF1A, MAP1S, Chemosensitivity, Autophagy, Keap1-Nrf2, A549/DDP

How to Cite This Article: Wei C, Huang R. RASSF1A Enhances Cisplatin Sensitivity in Non-Small Cell Lung Cancer via MAP1S-Dependent Autophagy Activation and Keap1-Nrf2 Pathway Suppression. Pharm Sci Drug Des. 2025;5:225-41. https://doi.org/10.51847/LtpbiPo3mC

Introduction

Lung cancer is the main cause of cancer-related deaths worldwide, with non-small cell lung cancer (NSCLC) accounting for roughly 80–85% of cases [1, 2]. Although chemotherapy remains a cornerstone of treatment, recent trials have explored combining standard chemotherapy with newer therapeutic agents [3]. Cisplatin (DDP), or cis-Diamineplatinum (II) dichloride, is one of the most widely used and effective drugs for treating advanced NSCLC [4–7]. However, its effectiveness is often compromised due to either inherent or acquired resistance in cancer cells, resulting in a low 5-year survival rate of under 25% and a local disease recurrence in nearly half of the patients [8, 9]. This chemoresistance remains a major obstacle to effective NSCLC therapy, highlighting the need to understand its molecular underpinnings [10].

Autophagy, classified as type II programmed cell death, serves as an alternative mechanism for cell death and can inhibit tumor growth [11]. Studies have shown that autophagy is a crucial process in regulating cell survival and death in NSCLC, indicating its importance in cancer progression [12]. Despite this, the exact role of autophagy in mediating chemoresistance in NSCLC is not fully understood. Deciphering autophagic pathways in specific cancers and treatment contexts is essential for improving chemotherapy outcomes.

© 2025 Pharmaceutical Sciences and Drug Design

The tumor suppressor RASSF1A is frequently silenced in various human cancers [13]. Research has demonstrated that while RASSF1A is expressed in normal tissues, its levels are reduced in NSCLC [14]. Beyond its tumor-suppressive functions, RASSF1A participates in regulating autophagy [15, 16]. Moreover, RASSF1A has been shown to interact with Microtubule-associated protein 1S (MAP1S), a key regulator of autophagy initiation, in hepatocellular carcinoma [17]. However, its role in autophagy-related chemoresistance in NSCLC remains poorly characterized. This study aims to investigate how RASSF1A-mediated autophagy influences NSCLC response to chemotherapy and to uncover the molecular mechanisms involved.

Here, we show that RASSF1A contributes to chemotherapy resistance in NSCLC in both in vitro and in vivo models. Mechanistically, RASSF1A regulates MAP1S and promotes autophagy, which in turn enhances NSCLC chemosensitivity. We propose a novel mechanism in which RASSF1A mediates DDP resistance via MAP1S-driven activation of the Keap1-Nrf2 pathway. These findings suggest that targeting RASSF1A may provide a promising approach to overcome DDP resistance in NSCLC patients.

Materials and Methods

Ethical statement

All animal and tissue studies were approved by the ethics committee of Harbin Medical University Affiliated Tumor Hospital. Animal experiments were performed in compliance with Harbin Medical University regulations on laboratory animals. Written informed consent was obtained from all participants, and ethical approval was granted by the hospital. Efforts were taken to minimize animal discomfort.

Clinical sample collection

A total of 56 fresh NSCLC tumor samples and corresponding adjacent normal tissues were collected from patients at Harbin Medical University. Tissues were immediately frozen in liquid nitrogen and stored at −80°C. All cases were adenocarcinomas. Inclusion criteria were: (1) primary NSCLC with no recurrence, (2) no prior chemotherapy, radiotherapy, or other treatments, (3) diagnosis confirmed by professional pathologists based on histopathological criteria, (4) no other malignancies, and (5) complete clinical and follow-up data.

Public database analysis

Data on RASSF1A expression in NSCLC patients were obtained from the Gene Expression Profiling Interactive Analysis (GEPIA, http://gepia.cancer-pku.cn/#index) using the parameters RASSF1A and LUAD.

Cell culture and transfection

Human NSCLC A549 cells and cisplatin-resistant A549/DDP cells were sourced from the American Type Culture Collection (Manassas, VA, USA). Both cell types were grown in RPMI-1640 medium supplemented with 10% fetal bovine serum and 100 μg/mL penicillin-streptomycin. To sustain the resistance of A549/DDP cells, 1 μg/mL cisplatin (Sigma-Aldrich, Merck KGaA, Darmstadt, Germany) was continuously included in their culture. All cells were incubated at 37°C under a 5% CO_2 humidified atmosphere.

For gene manipulation, A549/DDP cells were transfected using Lipofectamine 2000 (Thermo Fisher Scientific, Waltham, MA, USA) with plasmids or siRNAs including pCDNA3.1-RASSF1A, si-RASSF1A, and pCDNA3.1-MAP1S, along with their respective negative controls, pCDNA3.1 and si-NC (Genepharma, Shanghai, China). The experimental groups were designed to assess individual and combined effects of these genes and cisplatin treatment, including: pCDNA3.1-RA, si-RA, pCDNA3.1-MA, pCDNA3.1, si-NC, DDP alone, and combinations such as pCDNA3.1 + DDP, pCDNA3.1-RA + DDP, pCDNA3.1-MA + DDP, pCDNA3.1-MA + si-RA, pCDNA3.1-MA + si-RA + DDP, and pCDNA3.1-MA + DDP + 1 μM bardoxolone methyl (Nrf2 activator; Selleck, Shanghai, China). Negative control cells were included in all assays.

Cell viability assay (CCK-8)

Cells were plated at 5×10^3 per well in 96-well plates and allowed to attach for 24 hours. CCK-8 reagent was added to each well and incubated for 4 hours at 37°C. The optical density at 450 nm was recorded using a microplate reader, and experiments were performed in triplicate. Cell viability was calculated as: (OD of treated cells / OD of control cells) × 100%.

EdU proliferation assay

For proliferation analysis, cells were seeded at 1×10^5 per well in 96-well plates and incubated with 50 μM EdU (Sigma-Aldrich, Merck KGaA, Darmstadt, Germany) for 2 hours. After fixation for 30 minutes at room temperature, cells were treated with 2 mg/mL glycine for 5 minutes and washed with PBS. Following permeabilization, cells were incubated with Apollo reaction solution for 30 minutes in the dark and counterstained with DAPI for 30 minutes. Fluorescent images were captured using an Olympus fluorescence microscope (Tokyo, Japan).

Co-immunoprecipitation (Co-IP) assay

A549/DDP cells were lysed in RIPA buffer containing protease inhibitors at 4°C and centrifuged at 12,000 rpm for 15 minutes. Protein concentrations in the supernatant were measured with a BCA assay and adjusted to 2 μg/μL. Proteins were incubated overnight at 4°C with 10 μL of specific antibodies, while control samples received 10 μL of anti-IgG. Protein G agarose (30 μL) was added for overnight incubation at 4°C with rotation. After centrifugation at 14,000 g for 1 minute, beads were washed 3–5 times with RIPA buffer, resuspended in 30 μL of 2× Laemmli buffer, and heated at 100°C for 5 minutes. Supernatants were collected for Western blot analysis. Antibodies used included RASSF1A (ab31369, Abcam, UK), MAP1S (sc-517,081, Santa Cruz, USA), and anti-IgG (Thermo Fisher Scientific, USA).

Animal experiments

Four-week-old BALB/c-A nude mice were obtained from Hunan SJA Laboratory Animal Co., Ltd (Changsha, China) and maintained under specific pathogen-free conditions with a 12-hour light/dark cycle, providing unrestricted access to food and water. After one week of acclimatization, mice were randomly assigned to receive subcutaneous injections in the right dorsal flank with 1×10^6 A549/DDP cells. The injected cells were either untreated, transfected with the empty vector pCDNA3.1, or transfected with pCDNA3.1-RASSF1A (Hanheng, Shanghai, China), with six mice per group. Beginning the next day, mice were administered cisplatin intraperitoneally at 3.0 mg/kg, three times per week for a total of four weeks. At the end of the treatment period, mice were euthanized, and tumor tissues were collected, weighed, and processed for further analysis.

Quantitative reverse transcription PCR (qRT-PCR)

Total RNA was isolated from cultured cells or excised tumor tissues using TRIzol reagent (Invitrogen, Carlsbad, CA, USA) according to the manufacturer's protocol. RNA was converted into complementary DNA (cDNA) using a cDNA synthesis kit (Toyobo, Osaka, Japan), and concentrations were determined spectrophotometrically (Shimadzu, Kyoto, Japan). Quantitative PCR was performed with SYBR Green PCR Master Mix (Toyobo, Osaka, Japan) on an Applied Biosystems Prism 7300 system. Cycling conditions consisted of an initial denaturation at 95°C for 5 minutes, followed by 40 cycles of 95°C for 10 seconds, 60°C for 10 seconds, and 72°C for 20 seconds. Relative expression levels were calculated using the $2^{-\Delta\Delta Ct}$ method. The primers employed in this study are listed in **Table 1**.

Table 1. Primer Sequence for Quantitative Reverse Transcription Polymerase Chain Reaction to Determine the Expression Levels of RASSF1A, MAP1S, and GAPDH

Name	Primer
RASSF1A	F: 5′-CGCGCATTGCAAGTTCACC-3’
	R: 5′-AAGGTCAGGTGTCTCCCACT-3’
MAP1S	F: 5′-TCCTCACCTACGTCCTGGAG-3’
	R: 5′-CTGGAGAAGGTGGCAGAGTG-3’
GAPDH	F: 5′-TCTTGTGCAGTGCCAGCCT-3’
	R: 5′-TGAGGTCAATGAAGGGGTCG-3’

Abbreviations: MAP1S, microtubule-associated protein 1S; F, forward; R, reverse.

Western blot analysis

Cells were lysed using RIPA buffer supplemented with protease and phosphatase inhibitors. The lysates were centrifuged at 13,000 rpm for 30 minutes at 4°C. Tumor tissues were homogenized on ice in lysis buffer for 30

minutes and then centrifuged at 12,000 rpm for 5 minutes at 4°C. Protein concentrations in the supernatants were measured using a BCA assay kit. Equal amounts of protein were separated by SDS-PAGE and transferred onto membranes. Membranes were incubated overnight at 4°C with primary antibodies, followed by three washes with PBST. Secondary antibodies were applied for 30 minutes at room temperature, and after four additional washes, protein bands were visualized using an ECL detection system (GE Healthcare, Beijing, China).
Primary antibodies included GAPDH (ab181602), RASSF1A (ab31369), p62 (ab109012), LC3I/LC3II (ab51520), Nrf2 (ab62352) (Abcam, Cambridge, UK), MAP1S (sc-517081, Santa Cruz, Dallas, USA), and goat anti-rabbit IgG (Beijing ComWin Biotech Co., Ltd).

Immunofluorescence staining
Cells were fixed in 4% paraformaldehyde, washed three times with PBS, and permeabilized with 1% Triton X-100 for 25 minutes. After blocking with 5% bovine serum albumin for 45 minutes, cells were incubated with primary antibodies at 4°C overnight. Following three PBS washes, cells were treated with DyLight 488-conjugated goat anti-rabbit secondary antibody for 2 hours at room temperature. Nuclei were counterstained with DAPI (Beyotime Institute of Biotechnology), and fluorescence images were captured using a Nikon microscope (Japan).

Immunohistochemistry
Tumor tissues were fixed in 4% paraformaldehyde for 48 hours, embedded in paraffin, and sectioned at 4 μm. Sections were baked for 20 minutes, deparaffinized with xylene, and rehydrated in distilled water. After PBS washes, endogenous peroxidase activity was blocked with 3% H_2O_2 for 10 minutes. Antigen retrieval was performed, and sections were blocked with normal goat serum for 20 minutes at room temperature. Ki-67 (ab16667, 1:200; Abcam, Cambridge, MA, USA) primary antibody was applied overnight at 4°C. After three PBS washes, sections were incubated with secondary antibody for 1 hour at room temperature. Diaminobenzidine (DAB) was used for color development, nuclei were counterstained with hematoxylin for 3 minutes, and sections were dehydrated, cleared, and mounted. The proportion of positive cells was quantified.

TUNEL assay
Paraffin sections (4 μm) were deparaffinized with xylene and rehydrated through graded ethanol series. Apoptotic cells were detected using a TUNEL assay kit (ZK-8005; ZSJQB Co. Ltd., Beijing, China). Five random fields per section were examined under an Olympus microscope (Tokyo, Japan). Cells displaying brown or brownish-yellow staining with typical apoptotic morphology were counted as apoptotic. The apoptosis index (AI) was calculated as: AI = (number of TUNEL-positive cells / total number of cells) × 100%.

Statistical analysis
All data were analyzed using GraphPad Prism 7. Values are presented as mean ± standard deviation. Differences between two groups were assessed with Student's t-test, while comparisons among multiple groups were performed using one-way ANOVA followed by Dunnett's post hoc test. Kaplan–Meier analysis evaluated the association between RASSF1A expression and overall survival in NSCLC patients. The relationship between RASSF1A levels, pathological grade, and KPS scores was analyzed using chi-square tests, and associations with age at diagnosis were assessed by Student's t-test. A P-value < 0.05 was considered statistically significant.

Results and Discussion

RASSF1A expression is linked to clinical features and prognosis in NSCLC
To investigate the clinical significance of RASSF1A in NSCLC, we first analyzed its expression in tumor versus normal tissues using the GEPIA database. Tumor samples displayed a significant reduction in RASSF1A compared with normal tissues **(Figure 1a)**, ($P < 0.05$). To confirm these observations, we measured RASSF1A mRNA and protein levels in NSCLC specimens along with adjacent normal tissues. Both analyses demonstrated a marked decrease of RASSF1A in tumor tissues **(Figures 1b and 1c)** ($P < 0.05$).
We next evaluated the clinicopathological characteristics of 56 NSCLC patients, including age at diagnosis, tumor size, histological grade, and KPS score. Patients were divided into two groups based on RASSF1A expression relative to the mean value: 28 patients with expression below the average formed the RASSF1A Low group, while

the remaining 28 constituted the RASSF1A High group. Statistical analysis revealed no association between RASSF1A levels and patient sex (P = 0.7875) or age at diagnosis (P = 0.6289). In contrast, low RASSF1A expression was significantly correlated with larger tumors (P = 0.0151), higher pathological grade (P = 0.0135), reduced KPS scores (P = 0.0306), advanced TNM stage (P = 0.0315), presence of distant metastasis (P = 0.0143), and lymph node involvement (P = 0.0066) **(Table 2).** Overall, patients with lower RASSF1A levels tended to have more aggressive disease and poorer performance status.

Follow-up over 120 months showed a clear survival difference between groups. Kaplan–Meier analysis indicated that patients in the RASSF1A High group had a median survival of 109.5 months, while those in the Low group had a median survival of only 69.5 months **(Figure 1d)** (P = 0.0116). These results suggest that decreased RASSF1A expression is linked to worse postoperative outcomes in NSCLC patients.

Finally, we assessed MAP1S levels in tumors from both groups. Tumors from the RASSF1A Low group exhibited significantly lower MAP1S expression than those from the High group **(Figures 1e and 1f)** (P < 0.05). Collectively, these findings indicate that RASSF1A downregulation is associated with more aggressive NSCLC, poorer patient survival, and reduced MAP1S expression.

Table 2. The Association of RASSF1A Expressions with Clinical Pathological Characteristics of NSCLC Patients

Pathological Characteristics	RASSF1A Low	RASSF1A High	*P* values
Gender (Female/Male)	11/17	13/15	0.7875
Age (years)	51.12 ± 11.62	53.49 ± 9.35	0.6289
Tumor size (≤2 cm/>2 cm)	10/18	8/20	0.0151
Grade (1–2/3)	9/19	10/18	0.0135
KPS score (≥70/<70)	8/20	11/17	0.0306
TNM staging (I or II/III or IV)	9/19	18/10	0.0315
Distant metastasis (Absence/Presence)	11/17	21/7	0.0143
Lymphatic metastasis (Absence/Presence)	7/21	18/10	0.0066

Abbreviations: KPS score, Karnofsky performance scale score, KPS<70 points, means relative severe disease progression and KPS≥70 points refers to relative moderate disease progression; NSCLC, non-small cell lung cancer.

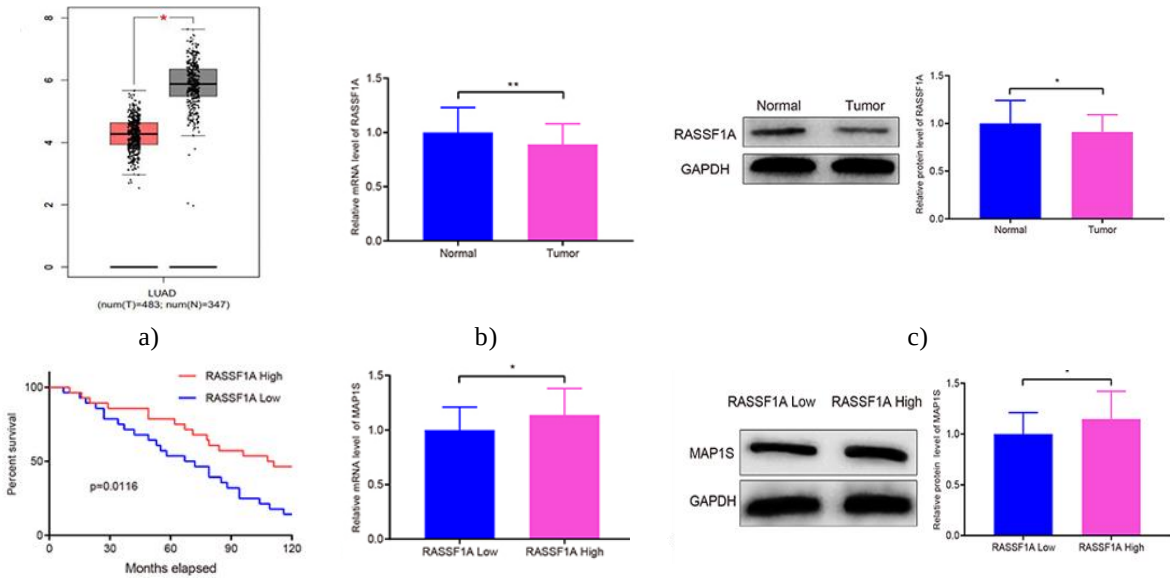

Figure 1. RASSF1A Correlates with Overall Survival in NSCLC Patients

Abbreviations: NSCLC, non-small cell lung cancer; MAP1S, microtubule-associated protein 1S.

Notes: RASSF1A expression in NSCLC tumor tissues was initially predicted using the GEPIA database (a). Validation of RASSF1A levels was performed by qRT-PCR and Western blot analyses (b and c). Kaplan–Meier survival curves were generated to evaluate the association between RASSF1A expression and overall

survival in NSCLC patients (d). MAP1S expression was quantified in tumor tissues using qRT-PCR and Western blotting (e and f). Data are expressed as mean ± standard deviation; *P < 0.05, **P < 0.01.

RASSF1A enhances cisplatin sensitivity in A549/DDP cells via autophagy induction

To investigate the role of RASSF1A in chemoresistance, A549 and cisplatin-resistant A549/DDP cells were treated with 10 μg/mL cisplatin. Cell viability assays showed that cisplatin significantly reduced survival in A549 cells compared with controls, whereas A549/DDP cells displayed minimal changes in viability under the same treatment **(Figures 2a and 2b).**

We next evaluated the inhibitory effects of varying concentrations of cisplatin on both cell lines. The IC50 for cisplatin in A549 cells was 17.61 μg/mL, while A549/DDP cells exhibited an IC50 of 46.72 μg/mL **(Figure 2c)**, confirming the higher resistance of A549/DDP cells.

Finally, RASSF1A expression was assessed in both cell types. qRT-PCR and Western blot analyses revealed that RASSF1A levels were markedly lower in A549/DDP cells than in parental A549 cells **(Figures 2d and 2e)** (P < 0.05), suggesting a potential link between reduced RASSF1A expression and cisplatin resistance.

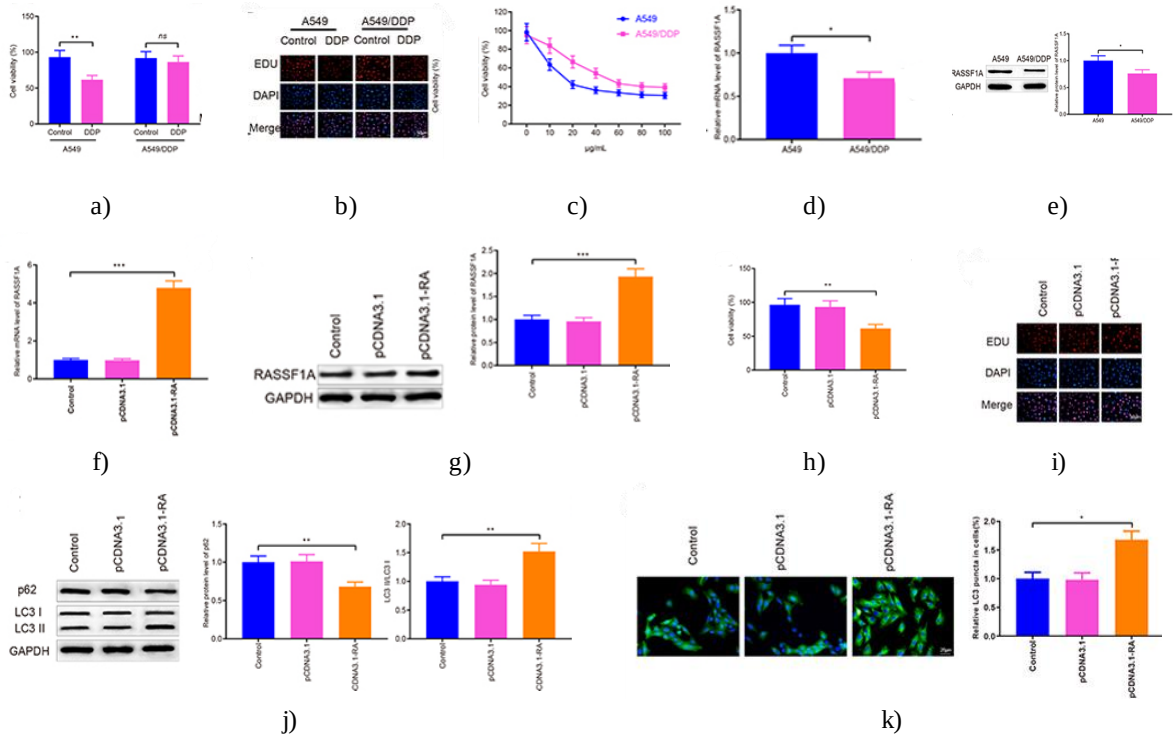

Figure 2. RASSF1A Enhances Autophagy and Restores Cisplatin Sensitivity in A549/DDP Cells

Abbreviations: DDP, cisplatin; MAP1S, microtubule-associated protein 1S; GFP, green fluorescent protein.

Notes: A549/DDP cells were transfected with pCDNA3.1-RASSF1A followed by DDP treatment, and cell viability was assessed using CCK-8 and EdU assays (a and b). The IC50 of DDP in A549 and A549/DDP cells was determined (c). RASSF1A expression was quantified by qRT-PCR and Western blot (d–g). Effects on cell viability were measured by CCK-8 and EdU assays (h and i). Autophagy markers p62, LC3II, and LC3I were analyzed by Western blot (j), and GFP-LC3 puncta were visualized by immunofluorescence (K). Data are presented as mean ± SD; *P < 0.05, **P < 0.01, ***P < 0.001

To examine the role of RASSF1A in NSCLC chemoresistance, A549/DDP cells were transfected with pCDNA3.1-RASSF1A. Assessment of transfection efficiency via qRT-PCR **(Figure 2f)** and Western blot **(Figure 2g)** confirmed a robust overexpression of RASSF1A in these cells (P < 0.001). Following transfection, cell viability assays demonstrated that cells overexpressing RASSF1A (pCDNA3.1-RA group) exhibited significantly reduced survival compared with controls (CCK-8) **(Figure 2h)**; (EdU) **(Figure 2i)** (P < 0.01). In contrast, cells transfected with the empty vector (pCDNA3.1) showed no significant changes in growth compared with the Control group (P > 0.05), suggesting that RASSF1A suppresses proliferation of cisplatin-resistant cells.

To explore the underlying mechanism, autophagy-related proteins were analyzed. Western blot results showed that overexpression of RASSF1A decreased p62 levels and increased the LC3II/LC3I ratio relative to controls **(Figure 2j)** ($P < 0.01$), indicating enhanced autophagy. Consistently, immunofluorescence analysis of GFP-LC3 puncta revealed a significant increase in puncta formation in the pCDNA3.1-RA group compared with controls **(Figure 2k)** ($P < 0.05$), further supporting RASSF1A-mediated autophagy induction.

Next, the effect of RASSF1A on cisplatin sensitivity was assessed. A549/DDP cells overexpressing RASSF1A were treated with DDP, and cell viability was measured. No significant differences were observed between the DDP + pCDNA3.1 group and DDP alone ($P > 0.05$). However, cells in the DDP + pCDNA3.1-RA group displayed markedly reduced survival compared with DDP alone **(Figures 3a and 3b)** ($P < 0.01$). Western blot analysis confirmed that DDP + pCDNA3.1-RA cells had lower p62 levels and higher LC3II/LC3I ratios compared with DDP alone, whereas no changes were observed in the DDP + pCDNA3.1 group **(Figure 3c)**

($P < 0.01$). Similarly, immunofluorescence revealed enhanced GFP-LC3 puncta in the DDP + pCDNA3.1-RA group relative to DDP alone **(Figure 3d)** ($P < 0.01$). Collectively, these results indicate that RASSF1A overexpression enhances autophagy and restores cisplatin sensitivity in resistant A549/DDP cells.

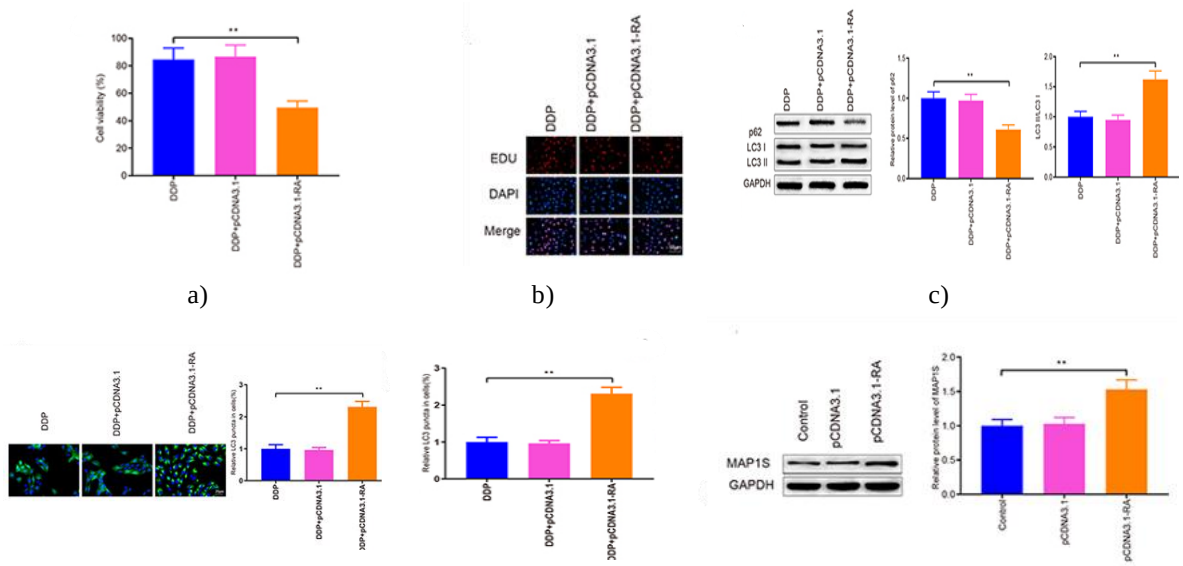

Figure 3. RASSF1A Enhances Autophagy and Restores Cisplatin Sensitivity in A549/DDP Cells

Abbreviations: GFP, green fluorescent protein; DDP, cisplatin.

Notes: Cell viability was assessed using CCK-8 and EdU assays (a and b). Autophagy markers p62, LC3II, and LC3I were analyzed by Western blot (c). GFP-LC3 puncta were visualized via immunofluorescence staining (d). MAP1S expression was quantified by qRT-PCR and Western blot (e and f); **P < 0.01.

To further understand the role of RASSF1A in chemoresistance, MAP1S levels were measured in A549/DDP cells following pCDNA3.1-RASSF1A transfection. Cells overexpressing RASSF1A (pCDNA3.1-RA group) showed significantly elevated MAP1S expression compared with control cells **(Figures 3e and 3f)**, ($P < 0.01$), whereas empty vector transfection (pCDNA3.1) had no effect on MAP1S levels ($P > 0.05$). These results suggest that RASSF1A may restore cisplatin sensitivity in A549/DDP cells by upregulating MAP1S and promoting autophagy.

MAP1S promotes autophagy and restores chemosensitivity in A549/DDP cells

We next analyzed MAP1S expression in parental A549 and cisplatin-resistant A549/DDP cells. Both qRT-PCR and Western blot analyses revealed that MAP1S was expressed at lower levels in A549/DDP cells compared with A549 cells **(Figures 4a and 4b)**, ($P < 0.05$). To clarify the functional role of MAP1S in NSCLC, A549/DDP cells were transfected with pCDNA3.1-MAP1S. Overexpression efficiency was confirmed by qRT-PCR and Western blot **(Figures 4c and 4d)** ($P < 0.001$).

Subsequent cell viability assays demonstrated that MAP1S overexpression significantly reduced the survival of A549/DDP cells (pCDNA3.1-MA group) compared with controls (CCK-8) **(Figure 4e)**, (EdU) **(Figure 4f)** ($P < 0.01$). In contrast, empty vector transfection did not affect cell viability relative to the Control group ($P > 0.05$), indicating that MAP1S inhibits A549/DDP cell proliferation.

To explore the mechanism, autophagy-related proteins were analyzed. Western blot showed decreased p62 levels and an increased LC3II/LC3I ratio in MAP1S-overexpressing cells relative to controls **(Figure 4g)** ($P < 0.01$), suggesting that MAP1S enhances autophagy. Immunofluorescence staining further confirmed increased GFP-LC3 puncta in the pCDNA3.1-MA group compared with the Control group **(Figure 4h)**, ($P < 0.01$). Collectively, these findings indicate that MAP1S promotes autophagy and improves cisplatin sensitivity in resistant NSCLC cells.

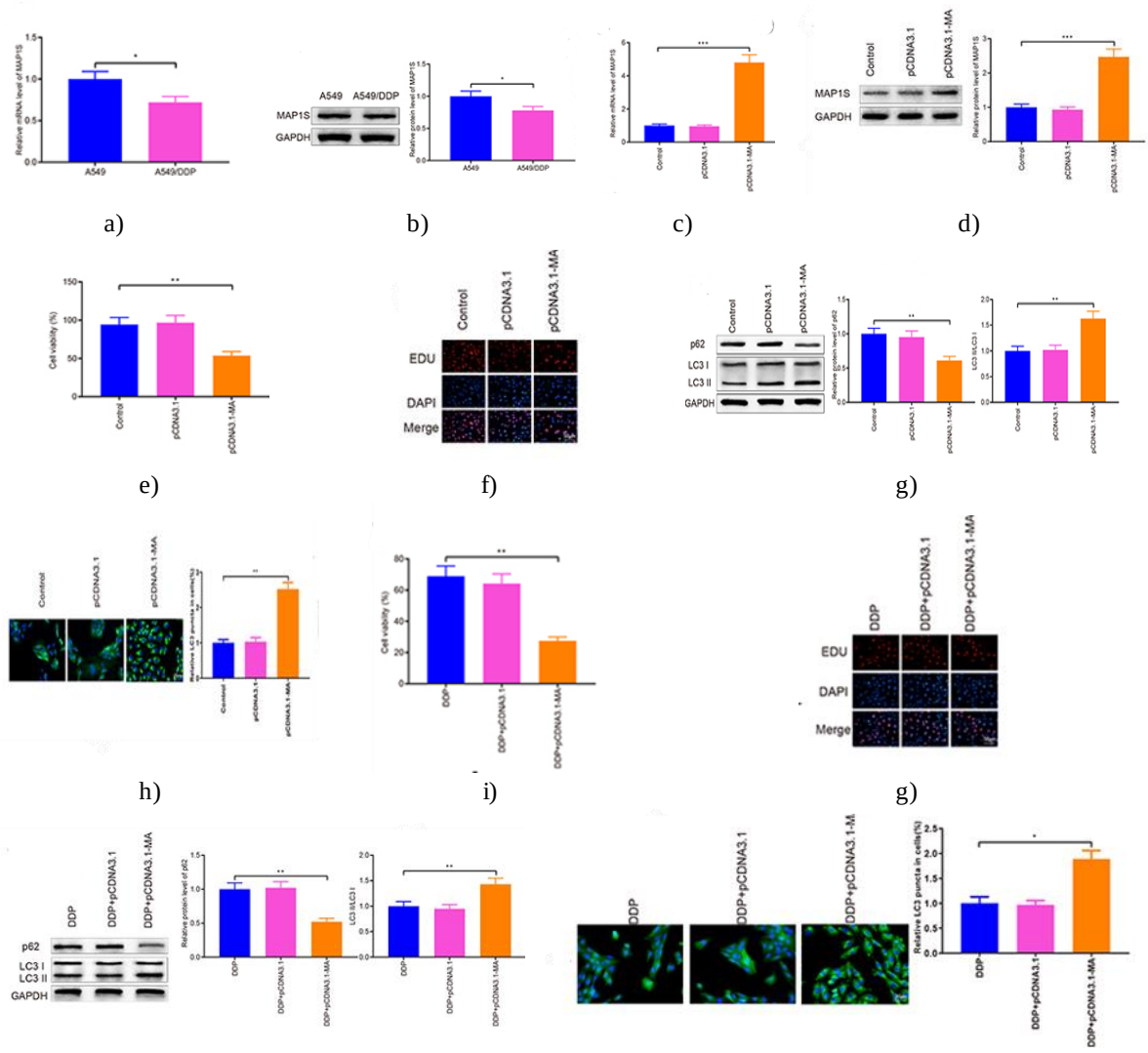

Figure 4. MAP1S Promotes Autophagy to Enhance Cisplatin Sensitivity in A549/DDP Cells

Abbreviations: DDP, cisplatin; MAP1S, microtubule-associated protein 1S; GFP, green fluorescent protein.

Notes: MAP1S expression in A549 and A549/DDP cells was measured by qRT-PCR and Western blot (A and B). After transfection with pCDNA3.1-MAP1S and DDP treatment, MAP1S levels were verified using qRT-PCR and Western blot (C and D). Cell viability was assessed using CCK-8 and EdU assays (E and F). Western blot was performed to determine p62, LC3II, and LC3I levels (G). GFP-LC3 puncta were visualized by immunofluorescence (H). Subsequent cell viability and autophagy analyses were conducted following combined MAP1S overexpression and DDP treatment (I–L). Data are expressed as mean ± SD; *$P < 0.05$, **$P < 0.01$, ***$P < 0.001$.

Cell viability assays revealed that MAP1S overexpression significantly decreased A549/DDP cell proliferation compared with control cells, while empty vector transfection had no effect **(Figures 4e and 4f)**, ($P < 0.01$). Consistent with this, Western blot analysis of autophagy markers showed a marked reduction in p62 and an increase in LC3II/LC3I ratio in MAP1S-overexpressing cells **(Figure 4g)**, ($P < 0.01$). Immunofluorescence staining of GFP-LC3 puncta further confirmed enhanced autophagy in MAP1S-transfected cells **(Figure 4h)**, ($P < 0.01$).

Next, to test whether MAP1S could sensitize resistant cells to cisplatin, A549/DDP cells overexpressing MAP1S were treated with DDP. Viability assays demonstrated that the combined MAP1S + DDP treatment markedly reduced cell survival compared with DDP alone **(Figures 4i and 4j)**, ($P < 0.01$). Western blot revealed that p62 was further suppressed and the LC3II/LC3I ratio increased in the MAP1S + DDP group versus DDP alone **(Figure 4k)**, ($P < 0.01$). Immunofluorescence confirmed an increase in GFP-LC3 puncta following MAP1S overexpression with DDP treatment **(Figure 4i)**, ($P < 0.05$). These results indicate that MAP1S enhances autophagy to restore cisplatin sensitivity in A549/DDP cells.

RASSF1A promotes autophagy through MAP1S to reverse chemoresistance

Clinical sample analysis revealed a significant positive correlation between RASSF1A and MAP1S expression in NSCLC tissues **(Figure 5a)**, ($P < 0.05$). Co-immunoprecipitation assays confirmed that RASSF1A physically interacts with MAP1S **(Figure 5b)**, ($P < 0.001$).

In vitro, knockdown of RASSF1A in A549/DDP cells using si-RASSF1A resulted in a significant reduction in both RASSF1A and MAP1S levels **(Figures 5c–5f)**, ($P < 0.01$). Co-transfection of si-RASSF1A with pCDNA3.1-MAP1S partially restored MAP1S expression. Functionally, these cells displayed higher viability compared with cells transfected with MAP1S alone **(Figures 5g and 5h)**, ($P < 0.05$), indicating that RASSF1A is required for MAP1S-mediated suppression of proliferation.

Western blot showed that autophagy induction by MAP1S was reduced when RASSF1A was silenced: p62 levels increased and LC3II/LC3I ratios decreased in the pCDNA3.1-MA + si-RASSF1A group relative to pCDNA3.1-MA alone **(Figure 5i)** ($P < 0.05$). Consistently, GFP-LC3 puncta were markedly decreased in the co-transfected cells **(Figure 5j)**, ($P < 0.05$). Together, these findings demonstrate that RASSF1A regulates MAP1S to activate autophagy, thereby enhancing cisplatin sensitivity in resistant NSCLC cells.

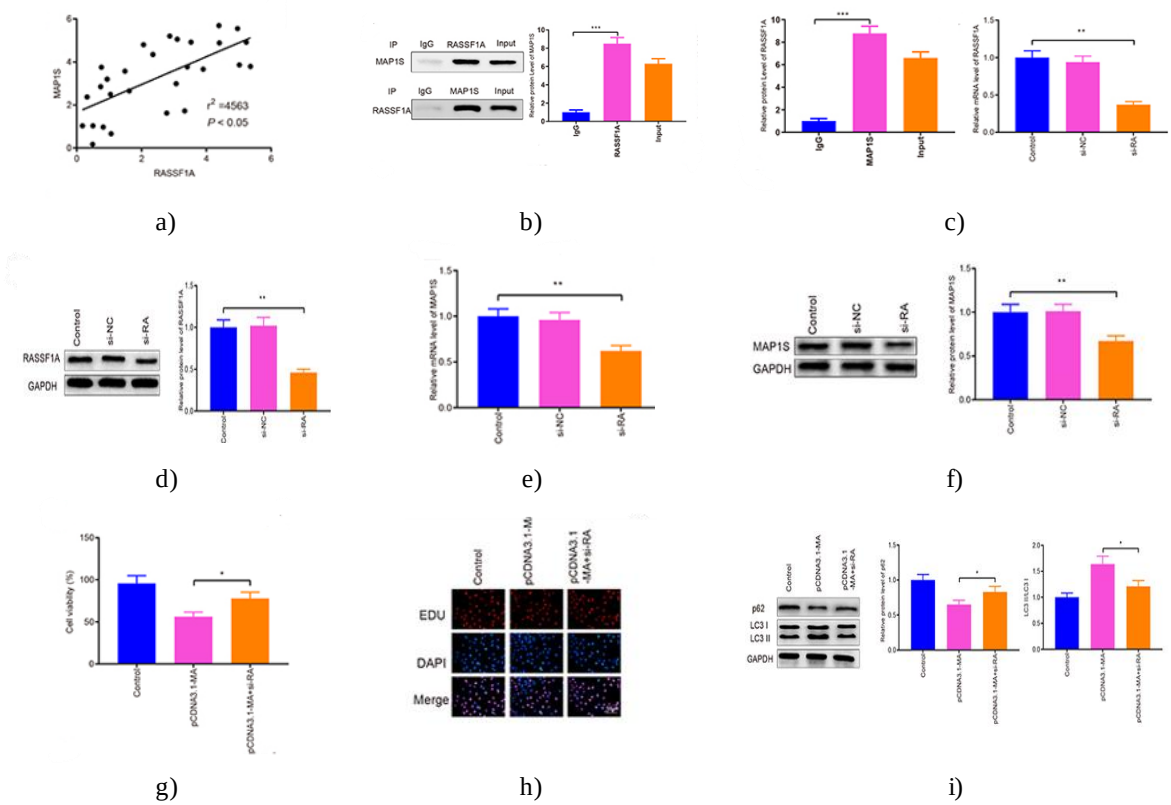

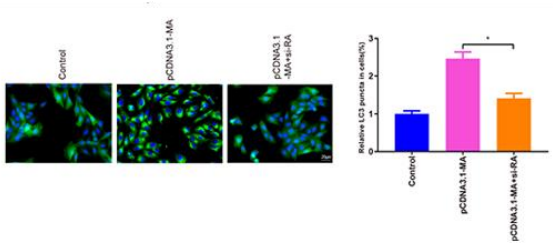

j)

Figure 5. RASSF1A Enhances Cisplatin Sensitivity in A549/DDP Cells via MAP1S-Mediated Autophagy Abbreviations: NSCLC, non-small cell lung cancer; MAP1S, microtubule-associated protein 1S; GFP, green fluorescent protein.

The relationship between RASSF1A and MAP1S in NSCLC tissues was evaluated, revealing a positive correlation **(Figure 5a)**, ($P < 0.05$). Co-immunoprecipitation confirmed a direct interaction between RASSF1A and MAP1S **(Figure 5b)**, ($P < 0.001$). In vitro, knockdown of RASSF1A using si-RASSF1A significantly reduced both RASSF1A and MAP1S expression levels, as shown by qRT-PCR and Western blot **(Figures 5c–5f)**, ($P < 0.01$).

To test the functional consequences of this interaction under chemotherapeutic stress, A549/DDP cells were co-transfected with si-RASSF1A and pCDNA3.1-MAP1S and then treated with cisplatin. Cell viability assays indicated that silencing RASSF1A partially rescued proliferation in MAP1S-overexpressing cells, resulting in higher survival compared with cells expressing MAP1S alone **(Figures 6a and 6b)**, ($P < 0.05$).

Analysis of autophagy markers revealed that p62 levels increased and the LC3II/LC3I ratio decreased in the pCDNA3.1-MA + si-RA + DDP group compared with the pCDNA3.1-MA + DDP group **(Figure 6c)**, ($P < 0.05$). Consistent with these findings, immunofluorescence showed reduced GFP-LC3 puncta in co-transfected cells **(Figure 6d)**, ($P < 0.05$), indicating diminished autophagic activity.

Taken together, these results suggest that RASSF1A facilitates autophagy through MAP1S, thereby enhancing cisplatin sensitivity in A549/DDP cells. Disruption of RASSF1A impairs MAP1S-mediated autophagy, reducing the chemosensitizing effect.

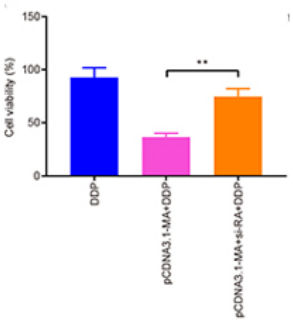

a)

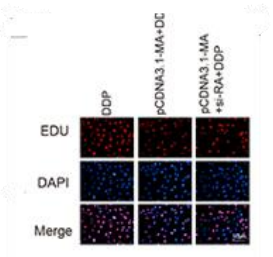

b)

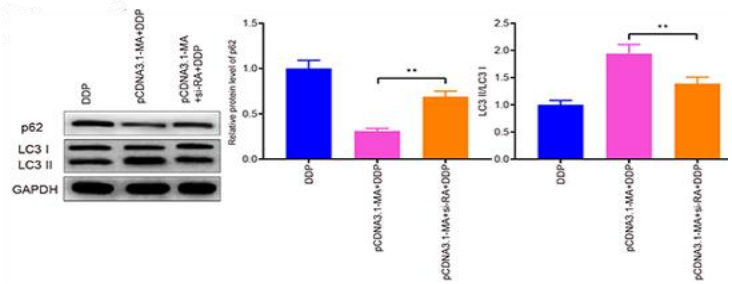

c)

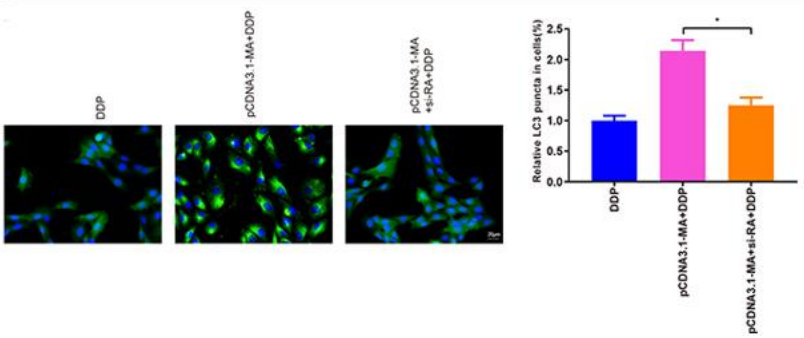

d)

Figure 6. RASSF1A Cooperates with MAP1S to Activate Autophagy and Enhance Cisplatin Sensitivity
Abbreviation: GFP, green fluorescent protein.

Cell viability was assessed using CCK-8 and EDU assays **(Figures 6a and 6b)**. The results showed that silencing RASSF1A in MAP1S-overexpressing A549/DDP cells partially rescued proliferation, leading to higher survival compared with cells expressing MAP1S alone ($P < 0.05$). Western blot analysis of autophagy markers revealed that the pCDNA3.1-MA + si-RASSF1A + DDP group had increased p62 levels and a lower LC3II/LC3I ratio relative to the pCDNA3.1-MA + DDP group **(Figure 6c)**, ($P < 0.05$). Immunofluorescence staining confirmed a reduction in GFP-LC3 puncta in the co-transfected cells **(Figure 6d)**, ($P < 0.05$), indicating that RASSF1A is required for MAP1S-mediated autophagy and cisplatin sensitization.

MAP1S promotes autophagy through the keap1-Nrf2 signaling pathway

To investigate the downstream mechanism by which MAP1S regulates autophagy, we examined the Keap1-Nrf2 pathway **(Figure 7a)**. Overexpression of RASSF1A or MAP1S alone (pCDNA3.1-RA and pCDNA3.1-MA groups) led to a significant reduction in Nrf2 protein levels compared with controls, suggesting suppression of the pathway. Notably, Nrf2 levels were elevated when RASSF1A was silenced in MAP1S-overexpressing cells (pCDNA3.1-MA + si-RASSF1A group) relative to MAP1S overexpression alone ($P < 0.05$). These results indicate that RASSF1A promotes autophagy and chemosensitivity in NSCLC cells by regulating MAP1S, which in turn modulates the Keap1-Nrf2 signaling axis.

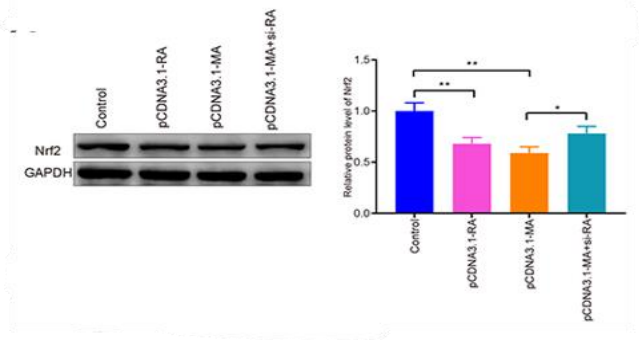

a)

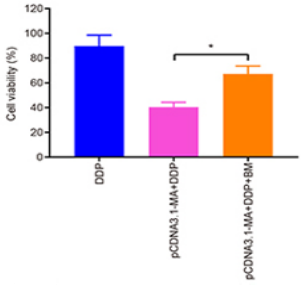

b)

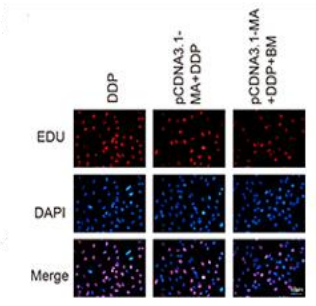

c)

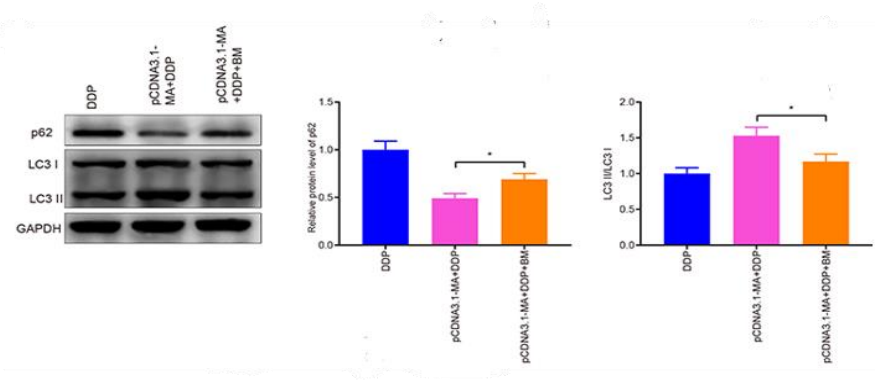

d)

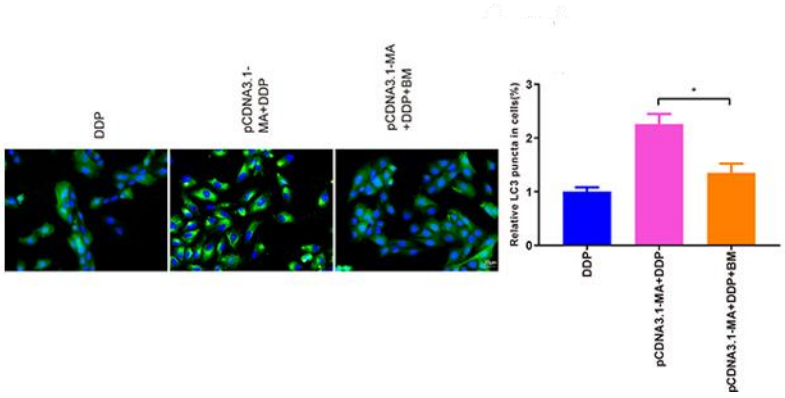

e)

Figure 7. MAP1S Enhances Chemosensitivity of A549/DDP Cells by Modulating the Nrf2 Pathway
Abbreviations: DDP, cisplatin; MAP1S, microtubule-associated protein 1S; GFP, green fluorescent protein.

To investigate whether the Nrf2 pathway mediates MAP1S-induced chemosensitivity, A549/DDP cells were transfected with pCDNA3.1-MAP1S and then co-treated with cisplatin and the Nrf2 activator bardoxolone methyl. Western blot analysis revealed that Nrf2 protein levels were suppressed in cells overexpressing MAP1S, whereas co-treatment with bardoxolone restored Nrf2 expression **(Figure 7a)**, ($P < 0.05$).
Cell viability assays using CCK-8 **(Figure 7b)** and EDU staining **(Figure 7c)** demonstrated that activating Nrf2 significantly increased survival in the pCDNA3.1-MA + DDP + BM group compared with the MAP1S-overexpressing cells treated with DDP alone ($P < 0.05$). Consistent with this, Western blot showed elevated p62 levels and reduced LC3II/LC3I ratios in the pCDNA3.1-MA + DDP + BM group relative to pCDNA3.1-MA + DDP group **(Figure 7d)**, ($P < 0.05$). Immunofluorescence analysis confirmed fewer GFP-LC3 puncta in cells treated with the Nrf2 activator **(Figure 7e)**, ($P < 0.05$). These findings indicate that MAP1S promotes autophagy and enhances chemosensitivity through inhibition of the Nrf2 pathway.

RASSF1A inhibits tumor growth in vivo and improves chemosensitivity
To validate the in vitro findings in vivo, a xenograft model was established by subcutaneously injecting A549/DDP cells overexpressing RASSF1A into nude mice. qRT-PCR and Western blot analyses of excised tumor tissues showed that both RASSF1A and MAP1S levels were significantly increased in the pCDNA3.1-RASSF1A group compared with the Blank group **(Figures 8a–8d)**, ($P < 0.01$), confirming efficient transfection and sustained overexpression in the tumors.

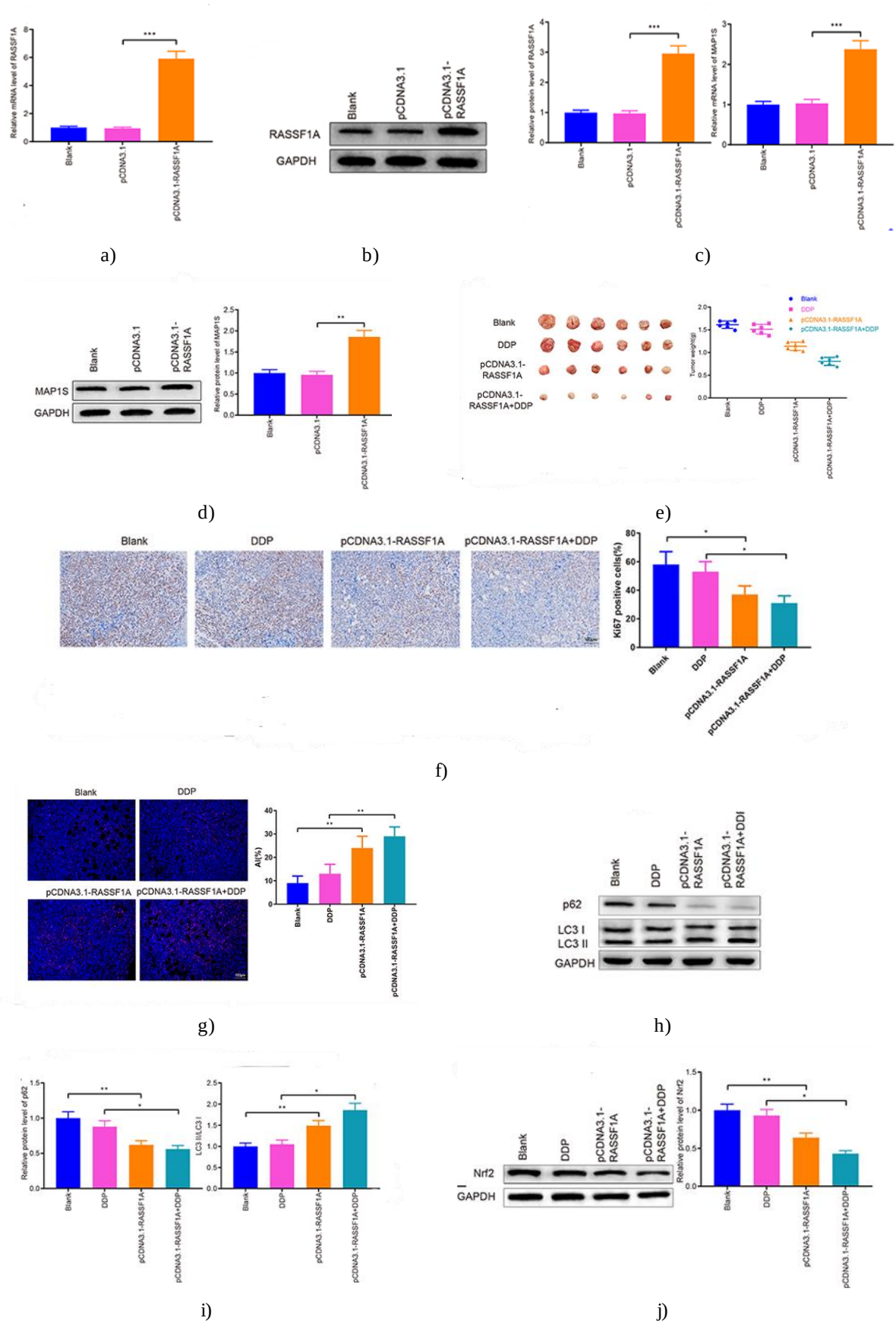

Figure 8. RASSF1A Suppresses Tumor Growth and Enhances Chemosensitivity In Vivo
Abbreviations: DDP, cisplatin; MAP1S, microtubule-associated protein 1S.

To evaluate the in vivo effects of RASSF1A, A549/DDP cells overexpressing RASSF1A were injected subcutaneously into nude mice, followed by DDP treatment. qRT-PCR and Western blot confirmed significant upregulation of RASSF1A and MAP1S in tumor tissues from the pCDNA3.1-RASSF1A group compared with the Blank group **(Figures 8a–8d)**, ($P < 0.01$).

Tumor weight measurements revealed that tumors in the pCDNA3.1-RASSF1A group were markedly smaller than those in the Blank group, and co-treatment with DDP further reduced tumor weight compared with DDP alone **(Figure 8e)**, ($P < 0.05$). Ki-67 immunohistochemistry showed fewer proliferating cells in the RASSF1A-overexpressing tumors, and the combination of RASSF1A overexpression and DDP further reduced Ki-67 positivity **(Figure 8f)**, ($P < 0.05$). TUNEL staining indicated that apoptosis was significantly higher in the pCDNA3.1-RASSF1A group, and co-treatment with DDP enhanced apoptotic index (AI) even further **(Figure 8g)**, ($P < 0.01$).

Western blot analysis demonstrated reduced p62 levels and an increased LC3II/LC3I ratio in tumors overexpressing RASSF1A, both with and without DDP treatment **(Figures 8h–8i)**, ($P < 0.05$). Nrf2 expression was also decreased in the pCDNA3.1-RASSF1A group and further suppressed in the RASSF1A + DDP group **(Figure 8j)**, ($P < 0.05$). Collectively, these results indicate that RASSF1A suppresses tumor growth, promotes apoptosis, and enhances chemosensitivity in vivo.

Autophagy can either facilitate or inhibit tumor development, and NSCLC cells typically exhibit elevated autophagy and rely on it for proliferation. In this study, we identified RASSF1A as an inducer of autophagy in NSCLC cells, thereby increasing their responsiveness to chemotherapeutic agents. We further clarified that RASSF1A enhances autophagy through MAP1S to suppress the Keap1–Nrf2 pathway, ultimately improving chemosensitivity. These results suggest a regulatory function of RASSF1A in autophagy and its relevance to NSCLC chemoresistance.

Autophagy has been widely recognized as a contributor to cancer cell chemoresistance [18–20], indicating that autophagy-related regulators may offer promising therapeutic targets for overcoming NSCLC drug resistance. Growing evidence supports that RASSF1A can act as an autophagy activator [17, 21], and this tumor suppressor has been implicated in modulating chemosensitivity across several cancer types [22–24]. However, no prior studies have specifically examined the relationship between RASSF1A and chemoresistance in NSCLC. In this work, we investigated the role of RASSF1A in NSCLC chemosensitivity. Using A549 cells and their cisplatin-resistant derivative A549/DDP as an in vitro model, we observed that RASSF1A expression was markedly reduced in A549/DDP cells compared with parental cells and negatively correlated with postoperative survival in NSCLC patients. Moreover, CCK-8 and EdU assays showed that combining RASSF1A overexpression with cisplatin resulted in significantly lower cell viability than cisplatin alone. Analysis of autophagy markers p62, LC3II, and LC3I further confirmed that RASSF1A promotes autophagy in A549/DDP cells. These findings indicate that RASSF1A may be involved in the molecular basis of cisplatin resistance in NSCLC, although its full biological role remains to be clarified.

MAP1S is an autophagy activator known to enhance both the formation and clearance of autophagosomes [25]. As a recently identified autophagy-associated protein, MAP1S has been shown to inhibit the progression of breast cancer [26, 27] and to suppress tumorigenesis by promoting autophagy [28]. Its tumor-inhibitory actions have also been demonstrated in hepatocellular carcinoma through enhancement of autophagy [29, 30]. In agreement with these findings, our experiments demonstrated that MAP1S restores chemosensitivity in A549/DDP cells by increasing autophagic activity.

A previous study identified MAP1S as a key interacting partner of RASSF1A [31], prompting us to hypothesize that RASSF1A suppresses NSCLC progression by inducing MAP1S-dependent autophagy. Correlation analyses confirmed that RASSF1A expression positively associates with MAP1S levels in clinical NSCLC samples, and their interaction was validated via CO-IP assays. Additionally, CCK-8 and EdU assays revealed that cells co-treated with RASSF1A silencing and MAP1S overexpression exhibited higher viability than those treated with RASSF1A overexpression alone. Since both RASSF1A and MAP1S regulate autophagosome formation and contribute to genome stability and tumor suppression [17, 26, 32], our protein-level analyses further verified that RASSF1A enhances autophagy by modulating MAP1S expression. When cells were subjected to combined RASSF1A knockdown and MAP1S overexpression followed by cisplatin treatment, cell viability increased significantly compared with the MAP1S-overexpression–plus–cisplatin group. Consistently, Western blotting showed increased p62 and reduced LC3II/LC3I ratios under these conditions. Collectively, these findings support that RASSF1A enhances NSCLC chemosensitivity by activating MAP1S-mediated autophagy.

We next investigated how RASSF1A regulates MAP1S to promote autophagy and increase chemosensitivity. The Keap1–Nrf2 pathway is a major protective and pro-survival signaling axis in mammalian cells, contributing to both innate and acquired drug resistance [33, 34]. Autophagy is closely linked to Nrf2 signaling, as MAP1S accelerates p62-dependent degradation of KEAP1 through the autophagy pathway [35]. In our study, Nrf2 protein levels were significantly reduced, indicating that RASSF1A may enhance autophagy via MAP1S to suppress Keap1–Nrf2 signaling and thereby overcome NSCLC chemoresistance. These mechanistic findings were further validated in vivo using a xenograft mouse model, where RASSF1A improved cisplatin chemosensitivity by enhancing autophagy and reducing tumor growth.

Conclusion

Our gain- and loss-of-function experiments demonstrate that RASSF1A enhances chemosensitivity in NSCLC by promoting autophagy. Mechanistic analyses further revealed that RASSF1A positively regulates MAP1S to trigger autophagy through inhibition of the Keap1–Nrf2 pathway, thereby increasing NSCLC cell susceptibility to chemotherapy both in vitro and in vivo. These results highlight the potential of targeting the RASSF1A –MAP1S axis as a strategy to improve chemotherapeutic responses in NSCLC.

Acknowledgments: Thanks for all the contributors and participants.

Conflict of Interest: None

Financial Support: This research was funded by the grants from Heilongjiang Postdoctoral Foundation (Grant No. LBH-Z18158); Reseach Fund of Postdoctor in Heilongjiang Province (LBH-Q15094), Health and Family Planning Commission Research Foundation of Heilongjiang Province (Grant No. 2016-091) and Natural Science Foundation of Heilongjiang Province (Grant No. H2016005).

Ethics Statement: None

References

1. Chen X, Wu Q, Chen Y, Zhang J, Ding J, Tang Z, et al. Diosmetin induces apoptosis and enhances the chemotherapeutic efficacy of paclitaxel in non-small cell lung cancer cells via Nrf2 inhibition. Br J Pharmacol. 2019;176(12):2079-94. doi:10.1111/bph.14652
2. Feng B, Zhang K, Wang R, Chen L. Non-small-cell lung cancer and miRNAs: novel biomarkers and promising tools for treatment. Clin Sci (Lond). 2015;128(10):619-34. doi:10.1042/CS20140530
3. Lazzari C, Karachaliou N, Bulotta A, Rosell R, Santarpia M. Combination of immunotherapy with chemotherapy and radiotherapy in lung cancer: is this the beginning of the end for cancer? Ther Adv Med Oncol. 2018;10:1758835918762094. doi:10.1177/1758835918762094
4. Dasari S, Tchounwou PB. Cisplatin in cancer therapy: molecular mechanisms of action. Eur J Pharmacol. 2014;740:364-78. doi:10.1016/j.ejphar.2014.07.025
5. Fennell DA, Summers Y, Cadranel J, Benepal T, Clement D, Lal R, et al. Cisplatin in the modern era: the backbone of first-line chemotherapy for non-small cell lung cancer. Cancer Treat Rev. 2016;44:42-50. doi:10.1016/j.ctrv.2016.01.003
6. Nakashima K, Murakami H, Omori S, Wakuda K, Ono A, Kenmotsu H, et al. Doublet chemotherapy with cisplatin and pemetrexed is associated with a favorable outcome in patients with advanced non-squamous non-small-cell lung cancer who are eligible for bevacizumab and maintenance therapy. Mol Clin Oncol. 2016;5(5):575-8. doi:10.3892/mco.2016.1001
7. Zhang YQ, Jiang LJ, Jiang SX, Qian J, Li J, Sun L, et al. Gefitinib with or without transarterial infusion chemotherapy (cisplatin) for large nonsmall cell lung cancer with epidermal growth factor receptor mutations. J Vasc Interv Radiol. 2019;30(7):1004-12. doi:10.1016/j.jvir.2018.12.705
8. Chaudhary KR, Yan SX, Heilbroner SP, Sonett JR, Stoopler MB, Shu CA, et al. Effects of beta-adrenergic antagonists on chemoradiation therapy for locally advanced non-small cell lung cancer. J Clin Med. 2019;8(5):575. doi:10.3390/jcm8050575

9. MacDonagh L, Gallagher MF, Ffrench B, Gasch C, Breen E, Gray SG, et al. Targeting the cancer stem cell marker, aldehyde dehydrogenase 1, to circumvent cisplatin resistance in NSCLC. Oncotarget. 2017;8(42):72544-63. doi:10.18632/oncotarget.19881
10. Makarova KS, Wolf YI, Alkhnbashi OS, Costa F, Shah SA, Saunders SJ, et al. An updated evolutionary classification of CRISPR-Cas systems. Nat Rev Microbiol. 2015;13(11):722-36. doi:10.1038/nrmicro3569
11. Kim M, Jung JY, Choi S, Lee H, Morales LD, Koh JT, et al. GFRA1 promotes cisplatin-induced chemoresistance in osteosarcoma by inducing autophagy. Autophagy. 2017;13(1):149-68. doi:10.1080/15548627.2016.1239676
12. Wang S, Xu X, Hu Y, Lei T, Liu T. Sotetsuflavone induces autophagy in non-small cell lung cancer through blocking PI3K/Akt/mTOR signaling pathway in vivo and in vitro. Front Pharmacol. 2019;10:1460. doi:10.3389/fphar.2019.01460
13. Dubois F, Bergot E, Zalcman G, Levallet G. RASSF1A, puppeteer of cellular homeostasis, fights tumorigenesis, and metastasis-an updated review. Cell Death Dis. 2019;10(12):928. doi:10.1038/s41419-019-2169-x
14. Chen T, Yang Z, Liu C, Wang L, Yang J, Chen L, et al. Circ_0078767 suppresses non-small-cell lung cancer by protecting RASSF1A expression via sponging miR-330-3p. Cell Prolif. 2019;52(2):e12548. doi:10.1111/cpr.12548
15. Del Re DP. Hippo signaling in the heart – non-canonical pathways impact growth, survival and function. Circ J. 2016;80(7):1504-10. doi:10.1253/circj.CJ-16-0426
16. Donninger H, Schmidt ML, Mezzanotte J, Barnoud T, Clark GJ. Ras signaling through RASSF proteins. Semin Cell Dev Biol. 2016;58:86-95. doi:10.1016/j.semcdb.2016.06.007
17. Li W, Yue F, Dai Y, He L, Wang Y, Zhang H, et al. Suppressor of hepatocellular carcinoma RASSF1A activates autophagy initiation and maturation. Cell Death Differ. 2019;26(8):1379-95. doi:10.1038/s41418-018-0211-7
18. He J, Yu JJ, Xu Q, Wang L, Zheng JZ, Liu LZ, et al. Downregulation of ATG14 by EGR1-MIR152 sensitizes ovarian cancer cells to cisplatin-induced apoptosis by inhibiting cyto-protective autophagy. Autophagy. 2015;11(2):373-84. doi:10.1080/15548627.2015.1009781
19. Huang Z, Zhou L, Chen Z, Nice EC, Huang C. Stress management by autophagy: implications for chemoresistance. Int J Cancer. 2016;139(1):23-32. doi:10.1002/ijc.29990
20. Shteingauz A, Boyango I, Naroditsky I, Hammond E, Gruber M, Doweck I, et al. Heparanase enhances tumor growth and chemoresistance by promoting autophagy. Cancer Res. 2015;75(18):3946-57. doi:10.1158/0008-5472.CAN-15-0037
21. Li W. Autophagy enhanced by RASSF1A suppresses diethylnitrosamine (DEN)-induced hepatocarcinogenesis [dissertation]. College Station (TX): Texas A&M University; 2017.
22. Guan HG, Xue WJ, Qian HX, Zhou XJ, Qin L, Lan J. RASSF1A expression inhibits cell growth and enhances cell chemosensitivity to mitomycin in BEL-7402 hepatocellular carcinoma cells. Chin Med J (Engl). 2009;122(11):1328-32.
23. Khandelwal M, Anand V, Appunni S, Seth A, Singh P, Mathur S, et al. Decitabine augments cytotoxicity of cisplatin and doxorubicin to bladder cancer cells by activating hippo pathway through RASSF1A. Mol Cell Biochem. 2018;446(1-2):105-14. doi:10.1007/s11010-018-3278-z
24. Li K, Yang J, Han X. Lidocaine sensitizes the cytotoxicity of cisplatin in breast cancer cells via up-regulation of RARβ2 and RASSF1A demethylation. Int J Mol Sci. 2014;15(12):23519-36. doi:10.3390/ijms151223519
25. Xu G, Yue F, Huang H, He L, Li W. Defects in MAP1S-mediated autophagy turnover of fibronectin cause renal fibrosis. Aging (Albany NY). 2016;8(5):977-85. doi:10.18632/aging.100957
26. Xie R, Wang F, McKeehan WL, Liu L. Autophagy enhanced by microtubule- and mitochondrion-associated MAP1S suppresses genome instability and hepatocarcinogenesis. Cancer Res. 2011;71(24):7537-46. doi:10.1158/0008-5472.CAN-11-2170
27. Shi M, Yao Y, Han F, Li Y, Li Y. MAP1S controls breast cancer cell TLR5 signaling pathway and promotes TLR5 signaling-based tumor suppression. PLoS One. 2014;9(1):e86839. doi:10.1371/journal.pone.0086839
28. Liu L, McKeehan WL, Wang F, Xie R. MAP1S enhances autophagy to suppress tumorigenesis. Autophagy. 2012;8(2):278-80.

29. Liu J, Zheng L, Ma L, Wang X, Yan T, Song G, et al. Oleanolic acid inhibits proliferation and invasiveness of Kras-transformed cells via autophagy. J Nutr Biochem. 2014;25(11):1154-60. doi:10.1016/j.jnutbio.2014.06.006
30. Yue F, Li W, Zou J, Jiang X, Liu G, Huang H, et al. Spermidine prolongs lifespan and prevents liver fibrosis and hepatocellular carcinoma by activating MAP1S-mediated autophagy. Cancer Res. 2017;77(11):2938-51. doi:10.1158/0008-5472.CAN-16-3462
31. Dallol A, Cooper WN, Al-Mulla F, Agathanggelou A, Maher ER, Latif F. Depletion of the Ras association domain family 1, isoform A-associated novel microtubule-associated protein, C19ORF5/MAP1S, causes mitotic abnormalities. Cancer Res. 2007;67(2):492-500. doi:10.1158/0008-5472.CAN-06-3604
32. Xie R, Nguyen S, McKeehan K, Wang F, McKeehan WL, Liu L. Microtubule-associated protein 1S (MAP1S) bridges autophagic components with microtubules and mitochondria to affect autophagosomal biogenesis and degradation. J Biol Chem. 2011;286(12):10367-77. doi:10.1074/jbc.M110.206532
33. Jaramillo MC, Zhang DD. The emerging role of the Nrf2-Keap1 signaling pathway in cancer. Genes Dev. 2013;27(20):2179-91. doi:10.1101/gad.225680.113
34. Kensler TW, Wakabayashi N, Biswal S. Cell survival responses to environmental stresses via the Keap1-Nrf2-ARE pathway. Annu Rev Pharmacol Toxicol. 2007;47:89-116. doi:10.1146/annurev.pharmtox.46.120604.141046
35. Liu P, Dodson M, Li H, Schmidlin CJ, Shakya A, Zhang DD, et al. Spermidine confers liver protection by enhancing NRF2 signaling through a MAP1S-mediated noncanonical mechanism. Hepatology. 2019;70(1):372-88.